

W BOSON PHYSICS AT THE FERMILAB TEVATRON*

JOHN ELLISON

Physics Department,
University of California,
Riverside, CA 92521, USA*(Received October 16, 2018)*

We present electroweak physics results from the DØ and CDF experiments using data from $p\bar{p}$ collisions at $\sqrt{s} = 1.8$ TeV. Measurements of the cross sections times branching ratios for W and Z production, the inclusive width of the W boson and the W boson mass are presented. Direct tests of the $WW\gamma$ and WWZ trilinear gauge boson couplings are also presented based on studies of diboson production.

PACS numbers: 14.70.Fm, 13.38.Be, 13.38.-b, 13.40.Em.

1. Introduction

The CDF and DØ detectors at the Fermilab Tevatron collider collected data during the 1992-93 run (“run 1a”) corresponding to integrated luminosities of ≈ 15 pb $^{-1}$ and ≈ 20 pb $^{-1}$ for DØ and CDF respectively. In the 1994-95 run (“run 1b”) data sets of ≈ 80 pb $^{-1}$ (DØ) and ≈ 90 pb $^{-1}$ (CDF) were collected. The large Tevatron data sets allow precise measurements of the W boson properties, such as its mass and width, and new studies of the physics of electroweak boson pair production.

In this paper we present selected recent results on W boson physics from the analysis of a subset of these data, concentrating mainly on electroweak physics. Theoretical aspects of W production at hadron colliders are covered in the talk by Stirling at this conference.

2. W and Z Production and the Inclusive Width of the W Boson

The measurement of the production cross-sections times branching ratios ($\sigma \cdot B$) for the W and Z bosons allows a determination of the width of

* Presented at the Cracow Epiphany Conference on the W Boson, 4-6 January 1997, Kraków, Poland.

the W boson and a comparison of W and Z boson production with QCD predictions. The latter are calculated to order α_s^2 and therefore, precision measurements of the cross sections are a test of radiative processes in QCD.

Measurements of the cross sections were made by DØ and CDF using the $W \rightarrow e\nu$, $Z \rightarrow ee$, $W \rightarrow \mu\nu$ and $Z \rightarrow \mu\mu$ decay channels. Events were selected from single lepton triggers and offline were required to contain a high p_T isolated lepton plus missing transverse energy (W events) or two high p_T isolated leptons (Z events). The DØ and CDF run 1a analyses are described in [1, 2].

Figure 1 shows the DØ preliminary run 1b transverse mass spectra for $W \rightarrow \ell\nu$ candidate events and the invariant mass spectra for $Z \rightarrow \ell\ell$ candidate events.

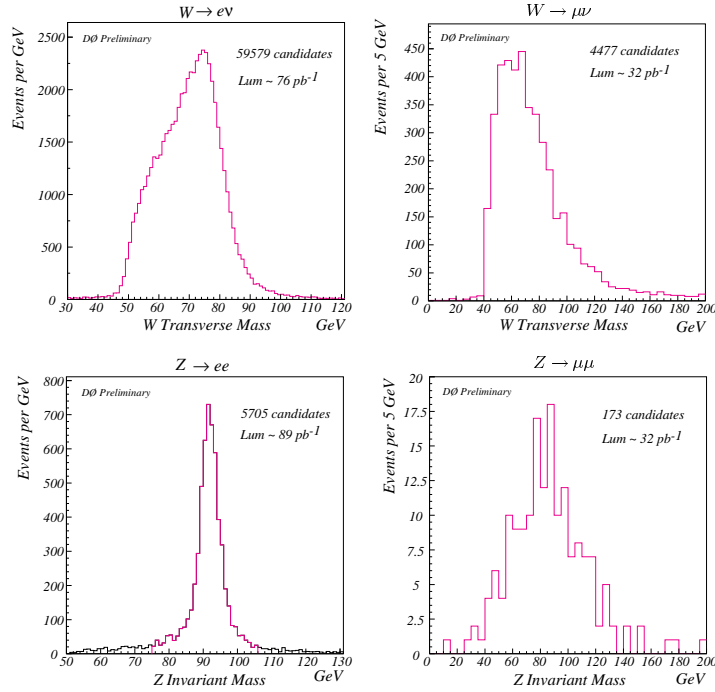


Fig. 1. Transverse mass and invariant mass distributions for the DØ W and Z candidate events from run 1b.

The values of $\sigma \cdot B$ were calculated by subtracting the background from the number of observed events and dividing by the acceptance, efficiency and integrated luminosity. The results are shown in Table 1 and are plotted in Fig. 2. The measurements agree well with the order α_s^2 QCD predictions (van Neerven *et al.* [3]) of $\sigma_W \cdot B(W \rightarrow \ell\nu) = 2.42^{+0.13}_{-0.11}$ nb and $\sigma_Z \cdot B(W \rightarrow \ell\nu) = 0.226^{+0.011}_{-0.009}$ nb, shown as the shaded bands in Fig. 2. The

CTEQ2M parton distribution functions [4], and the values $m_W = 80.23 \pm 0.18$ GeV/ c^2 and $m_Z = 91.188 \pm 0.002$ GeV/ c^2 were used to calculate the central values.

	DØ		CDF	
	e	μ	e	μ
W cand.	59579	4472	13796	6222
A_W (%)	43.4 ± 1.5	20.1 ± 0.7	34.2 ± 0.8	16.3 ± 0.4
ϵ_W (%)	70.0 ± 1.2	24.7 ± 1.5	72.0 ± 1.1	74.2 ± 2.7
Bkg (%)	8.1 ± 0.9	18.6 ± 2.0	14.1 ± 1.3	15.1 ± 2.2
$\int \mathcal{L}$ (pb $^{-1}$)	75.9 ± 6.4	32.0 ± 2.7	19.7 ± 0.7	18.0 ± 0.7
Z cand.	5702	173	1312	423
A_Z (%)	34.2 ± 0.5	5.7 ± 0.5	40.9 ± 0.5	15.9 ± 0.3
ϵ_Z (%)	75.9 ± 1.2	43.2 ± 3.0	69.6 ± 1.7	74.7 ± 2.7
Bkg (%)	4.8 ± 0.5	8.0 ± 2.1	1.6 ± 0.7	0.4 ± 0.2
$\int \mathcal{L}$ (pb $^{-1}$)	89.1 ± 7.5	32.0 ± 2.7	19.7 ± 0.7	18.0 ± 0.7

Table 1. Summary of DØ and CDF analyses and production cross section times branching ratio results for W and Z bosons. The symbols A , ϵ and Bkg are the acceptance, detection efficiency and background, respectively.

The inclusive width of the W boson is calculated using the measured ratio (R) of the W and Z $\sigma \cdot B$ values:

$$R = \frac{\sigma_W \cdot B(W \rightarrow \ell\nu)}{\sigma_Z \cdot B(Z \rightarrow \ell\ell)} \quad \text{with} \quad B(W \rightarrow \ell\nu) = \frac{\Gamma(W \rightarrow \ell\nu)}{\Gamma(W)}$$

Many common sources of error cancel in R , including the uncertainty in the integrated luminosity and parts of the errors in the acceptance and event selection efficiency. The theoretical calculation $\sigma_W/\sigma_Z = 3.33 \pm 0.03$ [3] and the LEP measurement $B(Z \rightarrow \ell\ell) = (3.367 \pm 0.0006)\%$ [5] are used to obtain $B(W \rightarrow \ell\nu)$. This measurement of $B(W \rightarrow \ell\nu)$ is then combined with a theoretical calculation [1, 6] of $\Gamma(W \rightarrow \ell\nu) = 225.2 \pm 1.5$ MeV to obtain an indirect measurement of the W inclusive width.

Figure 3 summarizes the measurements to date. The world average (excluding the preliminary DØ run 1b results) is $\Gamma(W) = 2.062 \pm 0.059$ GeV. This can be compared with the Standard Model (SM) prediction of 2.077 ± 0.014 GeV [1, 6] to set limits on non-standard decays of the W . At the 95% confidence level, the upper limit on the width due to non-standard decays (*e.g.* decays to heavy quarks or to SUSY particles such as charginos and neutralinos) is 109 MeV (*i.e.* approximately 5% of the W width).

The W width directly affects the shape of the transverse mass distribution in W events. The effect is most prominent at high values of m_T where

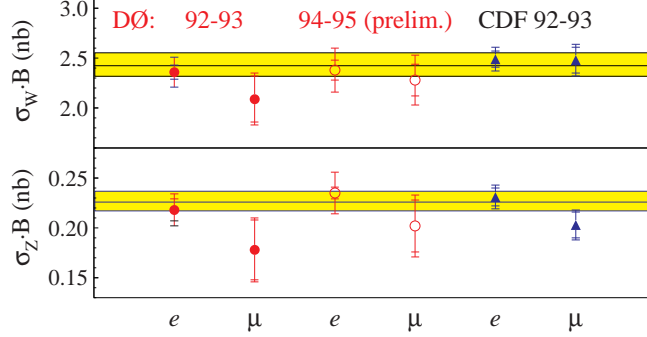


Fig. 2. Measurements of the W and Z inclusive cross-sections times branching ratios from DØ (circles) and CDF (triangles). Also shown are the SM theoretical predictions (shaded bands show central values and $\pm 1\sigma$ uncertainties).

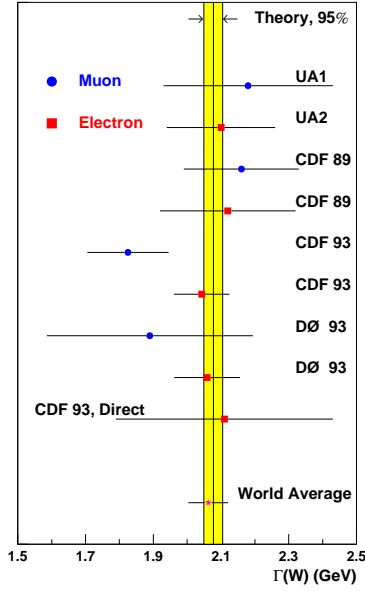


Fig. 3. Measurements of the W width from the Tevatron and CERN compared with the SM theoretical prediction.

the Breit-Wigner line shape dominates over the detector resolutions. CDF have utilized this fact to determine the W width from a binned likelihood fit to the transverse mass distribution in the region $m_T > 110 \text{ GeV}/c^2$ [7]. The result is $\Gamma_W = 2.11 \pm 0.28 \pm 0.16 \text{ GeV}$. This method is currently less precise than the indirect method described above but is relatively independent of SM assumptions.

3. Diboson Production and the Gauge Boson Couplings

The production of electroweak boson pairs at hadron colliders is particularly interesting since these processes probe the nature of the non-Abelian gauge boson self-couplings of the Standard Model (*i.e.* the $WW\gamma$ and WWZ couplings). These processes are also sensitive to deviations from the tree level SM couplings, which may arise due to compositeness of the W and Z bosons or radiative loop corrections to the vertex factors as shown in the examples of Fig. 4. To test the agreement with the SM and to eval-

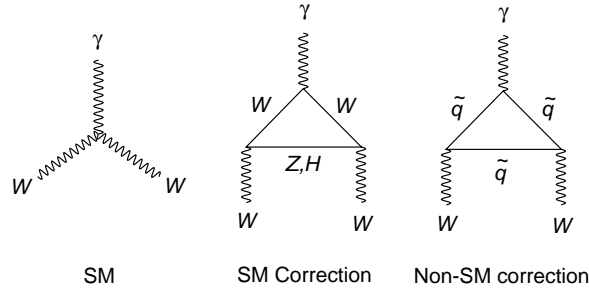


Fig. 4. Standard Model $WW\gamma$ vertex (left) and examples of loop corrections leading to deviations from the tree-level SM vertex functions.

uate the sensitivity to anomalous couplings the WWV ($V = \gamma, Z$) vertex is parametrized using the phenomenological effective Lagrangian of reference [8]. Assuming electromagnetic gauge invariance, and invariance under Lorentz and CP transformations the effective Lagrangian is reduced to a function of five dimensionless coupling parameters g_1^Z, κ_V , and λ_V . In the SM at tree level $g_1^Z = 1, \kappa_V = 1$ and $\lambda_V = 0$. Assuming that the coupling parameters for the $WW\gamma$ and WWZ vertices are equal, only two parameters remain:

$$\begin{aligned} \kappa_\gamma &= \kappa_Z = \kappa \quad (\text{or } \Delta\kappa \equiv \kappa - 1) \\ \lambda_\gamma &= \lambda_Z = \lambda. \end{aligned}$$

The coupling parameters are related to the lowest order terms in a multipole expansion of photon interactions with the W boson, *e.g.* the W magnetic dipole moment is given by $\mu_W = (e/2m_W)(1 + \kappa_\gamma + \lambda_\gamma)$.

All interaction Lagrangians with constant anomalous couplings violate unitarity at high energy. In the SM delicate cancellations ensure that unitarity is satisfied and anomalous couplings would destroy these cancellations leading to violation of unitarity. Therefore, all the coupling parameters must be modified to include form factors, *e.g.*

$$\Delta\kappa(\hat{s}) = \frac{\Delta\kappa^0}{(1 + \hat{s}/\Lambda^2)^n}$$

where $\Delta\kappa^0$ = value of coupling parameter at $\hat{s} = 0$, \hat{s} = square of the invariant mass of the partonic subprocess, $n = 2$ for a dipole form factor and Λ = form factor scale (a function of the scale of new physics).

3.1. $W\gamma$ Production and the $WW\gamma$ Coupling

The study of $W\gamma$ production at the Tevatron can be used to probe the $WW\gamma$ coupling [9]. The u - and t -channel Feynman diagrams for $p\bar{p} \rightarrow \ell\nu\gamma$ correspond to photon bremsstrahlung from an initial state quark, whereas the s -channel diagram is sensitive to the $WW\gamma$ vertex. Events in which a photon is radiated from the final state lepton from single W decay also result in the same $\ell\nu\gamma$ final state, but are suppressed by imposing a cut on the photon-lepton angular separation. Non-SM values of the $WW\gamma$ coupling result in an increase in the total cross-section and an enhancement of events with high- p_T photons. This is the experimental signature which is used by DØ [10] and CDF [11] to test for anomalous couplings.

In addition to the W selection criteria, a high- p_T isolated photon with $p_T > 10$ (7) GeV is required in the DØ (CDF) analyses, separated from the lepton by $\Delta R_{\ell\nu} > 0.7$ units in $\eta - \phi$ space. Photons are detected in the pseudorapidity range $|\eta| < 1.1$ for CDF and $|\eta| < 1.1$ or $1.5 < |\eta| < 2.5$ for DØ.

The numbers of signal events after background subtraction are compared with the SM predictions in Table 2. Note that the number of events is on the order of 100 for each experiment. The DØ measured cross section times branching ratio (with $E_T^\gamma > 10$ GeV and $\Delta R_{\ell\nu} > 0.7$) is $\sigma(W\gamma) \times B(W \rightarrow \ell\nu) = 11.3_{-1.5}^{+1.7}$ (stat) ± 1.5 (sys) pb compared with the SM prediction of $\sigma(W\gamma) \times B(W \rightarrow \ell\nu) = 12.5 \pm 1.0$ pb. Figure 5 shows the DØ p_T^γ distribution for the observed candidate events together with the SM signal prediction plus the sum of the estimated backgrounds. The number of observed events and the shapes of the distributions show no deviations from the expectations. The SM predictions for the number of events observed was obtained using the leading order $W\gamma$ event generator of Baur and Zeppenfeld [12] (using a K-factor of 1.34 to approximate higher order QCD effects) combined with Monte Carlo simulations of the DØ and CDF detectors.

In both experiments, limits on the $WW\gamma$ vertex coupling parameters are obtained from a binned maximum likelihood fit to the photon p_T distribution. In the electron channel run 1b analysis, DØ require the electron-photon-neutrino transverse cluster mass to be > 90 GeV/ c^2 . This cut suppresses radiative W decays and increases the sensitivity to anomalous couplings by about 10%. Figure 6 shows the 95% confidence level (CL) limits in the $\Delta\kappa - \lambda$ plane, for a form factor scale of $\Lambda = 1.5$ TeV. Varying only

	DØ 92.8 pb ⁻¹		CDF 67.0 pb ⁻¹	
	$W\gamma \rightarrow e\nu\gamma$	$W\gamma \rightarrow \mu\nu\gamma$	$W\gamma \rightarrow e\nu\gamma$	$W\gamma \rightarrow \mu\nu\gamma$
N_{data}	57	70	75	34
N_{bkg}	15.2 ± 2.5	27.7 ± 4.7	16.1 ± 2.4	10.3 ± 1.2
N_{sig}	$41.8^{+8.8}_{-7.5}$	$42.3^{+9.7}_{-8.3}$	$58.9 \pm 9.0 \pm 2.6$	$23.7 \pm 5.9 \pm 1.1$
N_{SM}	43.6 ± 3.1	38.2 ± 2.8	53.5 ± 6.8	21.8 ± 4.3

Table 2. The number of candidate $W\gamma$ events observed in the DØ and CDF analyses (N_{data}). N_{bkg} is the estimated background and N_{sig} is the number of signal events after background subtraction. Also shown is the SM prediction N_{SM} .

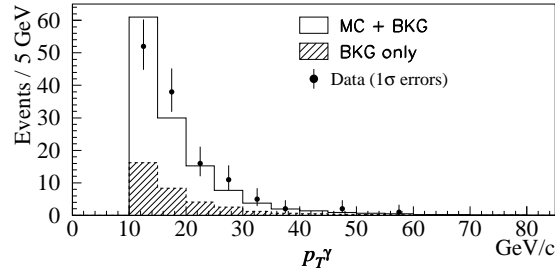


Fig. 5. Distribution of photon transverse energy p_T^γ for the DØ combined run 1a plus 1b analyses. The shaded areas represent the estimated background and the solid histograms are the expected signal from the Standard Model plus the estimated background.

one coupling at a time, the following limits are obtained at the 95% CL:

$$\begin{aligned} \text{DØ:} \quad & -0.9 < \Delta\kappa < 0.9 \quad (\text{for } \lambda = 0) \\ & -0.3 < \lambda < 0.3 \quad (\text{for } \Delta\kappa = 0) \end{aligned}$$

$$\begin{aligned} \text{CDF:} \quad & -1.8 < \Delta\kappa < 2.0 \quad (\text{for } \lambda = 0) \\ & -0.7 < \lambda < 0.6 \quad (\text{for } \Delta\kappa = 0) \end{aligned}$$

The possibility of a minimal U(1)-only coupling ($\kappa = \lambda = 0$) indicated by the star in Fig. 6 is ruled out at the 88% CL by the DØ measurement. This shows that the photon couples not only to the W electric charge but also to its weak isospin.

3.2. WW and WZ Production

DØ and CDF have searched for WW and WZ production using two decay modes: (a) the “dilepton” mode and (b) the “lepton plus jets” mode.

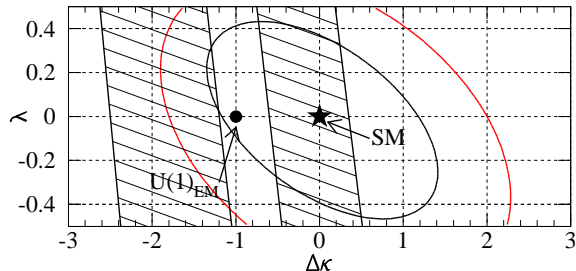


Fig. 6. 95% CL limits on the $WW\gamma$ couplings from DØ (inner ellipse) and CDF (outer ellipse). The shaded bands are the regions allowed by the CLEO 95% CL limits from the observation of $b \rightarrow s\gamma$ decays [13].

Both experiments have searched for WW production in the dilepton decay modes $e\nu e\nu$, $e\nu\mu\nu$ and $\mu\nu\mu\nu$ [14, 15]. In the preliminary DØ run 1b analysis, based on an integrated luminosity of 78.5 pb^{-1} , four events pass the event selection criteria. DØ set an upper limit on the cross section for $p\bar{p} \rightarrow WW$ of 41 pb at the 95% CL, estimated based on four candidate events and a total estimated background of 2.6 ± 0.4 events.

In the CDF analysis based on 108 pb^{-1} of data, a SM WW signal is observed above background. The event selection yields 5 events with a background of 1.2 ± 0.3 events. The measured WW cross section is $\sigma(p\bar{p} \rightarrow WW) = 10.2^{+6.3}_{-5.1} \pm 1.6 \text{ pb}$. The cross section for this process has been calculated to next to leading order by Ohnemus [16] with the result $\sigma_{SM}(p\bar{p} \rightarrow WW) = 9.5 \pm 1.0 \text{ pb}$.

The W pair production process is sensitive to the $WW\gamma$ and WWZ couplings, since the s -channel propagator can be a γ or Z . Anomalous couplings result in a higher cross section and an enhancement of events with high p_T W bosons. Due to the low statistics in this channel, only the total cross section is used in setting limits. Assuming $\Delta\kappa_Z = \Delta\kappa_\gamma$ and $\lambda_Z = \lambda_\gamma$, the limits obtained on $\Delta\kappa$ and λ are shown in Fig. 7.

In the lepton plus jets analyses DØ and CDF search for candidate events containing a high- p_T lepton, missing E_T and two jets with invariant mass consistent with the W or Z mass. CDF also accept events with two charged leptons and two jets resulting from $p\bar{p} \rightarrow WZ \rightarrow \ell^+\ell^-jj$. The data are dominated by background, mainly from W + jets events with $W \rightarrow e\nu$ and multijet production where one jet was misidentified as an electron and there was significant (mismeasured) missing E_T . The data are in good agreement with the expectations.

At large values of p_T^W the backgrounds are relatively small and it is in this region where anomalous couplings would enhance the cross section. CDF make a cut at $p_T^W > 200 \text{ GeV}$, where p_T^W is calculated from the p_T

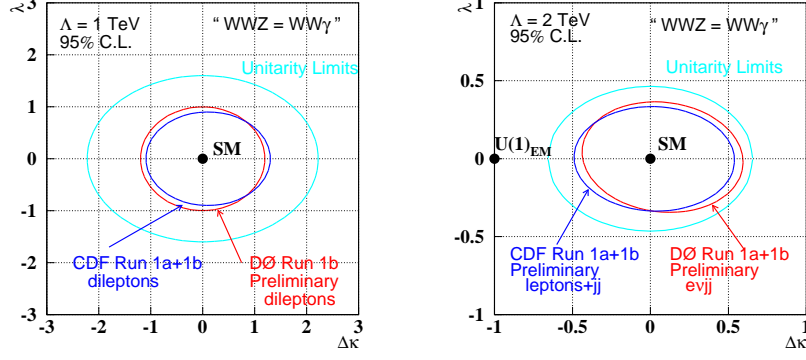


Fig. 7. 95% CL limits from DØ and CDF in the $\Delta\kappa - \lambda$ plane, assuming $g_1^Z = g_1^\gamma = 0$. Left: Limits from $WW \rightarrow \ell\nu\ell'\nu'$. Right: Limits from the $WW, WZ \rightarrow$ lepton(s) + jj decay modes.

of the dijet system. Limits on anomalous couplings are then derived by comparing the number of surviving events with the predicted number of events as a function of the anomalous coupling parameters, determined from the leading order calculation by Hagiwara, Woodside and Zeppenfeld [17] with a K-factor of 1.34.

DØ use a binned likelihood fit to the p_T^W spectrum above $p_T^W > 25$ GeV, where p_T^W is calculated from the p_T of the $e\nu$ system. The results, assuming the WWZ and $WW\gamma$ coupling parameters are equal, are shown in Fig. 7. At the 95% CL for $\Lambda = 2.0$ TeV, assuming $\Delta\kappa_Z = \Delta\kappa_\gamma, \lambda_Z = \lambda_\gamma$ the following limits are obtained:

$$\begin{aligned} \text{DØ:} \quad & -0.4 < \Delta\kappa < 0.6 \quad (\text{for } \lambda = 0) \\ & -0.3 < \lambda < 0.4 \quad (\text{for } \Delta\kappa = 0) \end{aligned}$$

$$\begin{aligned} \text{CDF:} \quad & -0.5 < \Delta\kappa < 0.6 \quad (\text{for } \lambda = 0) \\ & -0.4 < \lambda < 0.3 \quad (\text{for } \Delta\kappa = 0) \end{aligned}$$

Assuming SM $WW\gamma$ couplings and fixing $\lambda_Z = 0$, both experiments exclude the point $\kappa_Z = g_1^Z = 0$ at $> 99\%$ CL. This is direct evidence for a nonzero WWZ coupling.

4. Measurement of the W Boson Mass

The mass of the W boson m_W is one of the fundamental parameters of the SM. From the relation among the parameters of the SM we can write

m_W in terms of α , G , m_Z and Δr . Radiative corrections associated with the SM are contained in the Δr term, the largest contributions to Δr being proportional to m_t^2 and $\ln m_H$. Therefore, a precise determination of the W and top masses can be used to constrain the Higgs mass.

In $p\bar{p} \rightarrow W \rightarrow \ell\nu$ events at the Tevatron, the longitudinal component of the neutrino cannot be determined and therefore m_W is measured using the transverse mass defined by

$$m_T = \sqrt{2p_T^\ell p_T^\nu (1 - \cos \varphi^{\ell\nu})}$$

where $\varphi^{\ell\nu}$ is the angle between the lepton and neutrino in the transverse plane. The experimentally measured quantities are the lepton momentum and the transverse momentum of the recoil system \vec{p}_T^{had} . The transverse momentum of the neutrino is then inferred from these two observables:

$$\vec{E}_T = -\vec{p}_T^e - \vec{p}_T^{had} = -\vec{p}_T^e - \vec{p}_T^{rec} - \vec{u}_T(\mathcal{L})$$

The p_T of the recoil system is given by $\vec{p}_T^{had} = \vec{p}_T^{rec} + \vec{u}_T(\mathcal{L})$, where \vec{p}_T^{rec} is the transverse momentum of the W recoil and $\vec{u}_T(\mathcal{L})$ is the transverse energy flow of the underlying event, which depends on the luminosity. The latter two quantities are experimentally inseparable for W events.

The W mass is determined by generating Monte Carlo W events and fitting to the transverse mass distribution observed in the data. To correctly model the m_T distribution a precise knowledge of the response and resolution of the detector to charged leptons and the recoil particles is required. The response determines the position of the peak of the m_T distribution, while the resolution determines its width.

In CDF the momentum scale is determined by normalizing the measured $J/\psi \rightarrow \mu^+\mu^-$ mass peak to the world average value. The calorimeter energy scale is then determined from a comparison of the observed E/p distribution with a detailed Monte Carlo simulation. At DØ only $W \rightarrow e\nu$ events are used to measure m_W . The electromagnetic calorimeter energy scale is established using $Z \rightarrow e^+e^-$ events and calibrating against the LEP measurement of m_Z , with additional constraints from $J/\psi \rightarrow e^+e^-$ and $\pi^0 \rightarrow \gamma\gamma$ events.

In CDF the W p_T is modeled in the Monte carlo using the p_T distribution of Z events observed in the data. The recoil system is also taken from the Z data. The DØ experiment generates the W p_T using the double differential W production cross section in p_T and rapidity calculated to next to leading order by Ladinsky and Yuan [18]. Minimum bias events are used to model the underlying event. The response of the calorimeter to the hadronic recoil is determined from the balance in transverse momentum in Z events.

Figure 8 shows the transverse mass distributions for the data together with the best fit of the Monte Carlo for the muon and electron channel run 1a data (CDF) and the run 1b electron data (DØ).

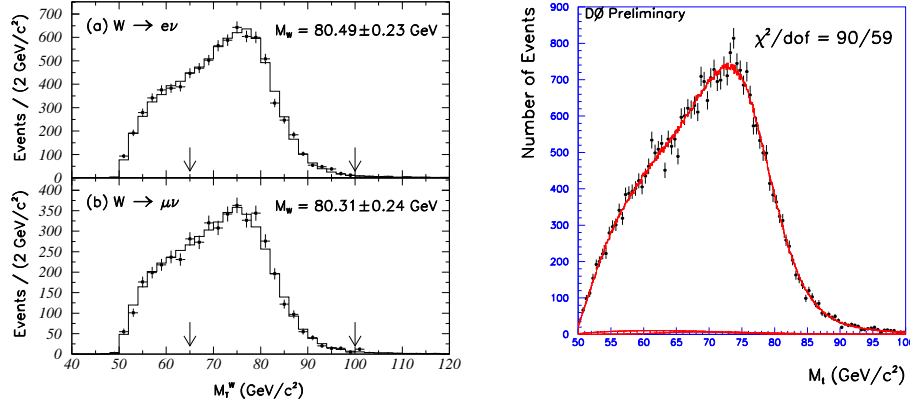


Fig. 8. Left: Transverse mass distributions from the CDF run 1a data. The points are the data and the histogram is the best fit to the data. The W mass is obtained by fitting in the mass range indicated by the arrows. Right: Transverse mass distribution from the DØ run 1b data. The W mass is obtained by fitting in the mass range $60 < m_T < 90$ GeV/c².

The W mass results are:

$$\begin{aligned} \text{DØ 1a: } m_W^e &= 80.350 \pm 0.140(\text{stat}) \pm 0.165(\text{syst}) \pm 0.160(\text{scale}) \text{ GeV}/c^2 \\ \text{DØ 1b: } m_W^e &= 80.380 \pm 0.070(\text{stat}) \pm 0.130(\text{syst}) \pm 0.080(\text{scale}) \text{ GeV}/c^2 \end{aligned}$$

$$\begin{aligned} \text{CDF 1a } W \rightarrow e\nu: m_W^e &= 80.490 \pm 0.145(\text{stat}) \pm 0.175(\text{sys}) \text{ GeV}/c^2 \\ \text{CDF 1a } W \rightarrow \mu\nu: m_W^\mu &= 80.310 \pm 0.205(\text{stat}) \pm 0.130(\text{sys}) \text{ GeV}/c^2 \end{aligned}$$

Table 3 lists the systematic errors on the individual measurements and the common errors.

Using the above results and combining with previous W mass measurements [19], a world average of $m_W = 80.356 \pm 0.125$ GeV/c² is obtained. The world average values of m_W and m_t are shown in Fig. 9. Also shown are the results from the indirect measurements from LEP and SLC and the predictions of the SM for various Higgs masses. The errors in the latter predictions are indicated by the width of the bands and are primarily due to the uncertainty in $\alpha(m_Z^2)$, the electromagnetic coupling strength at the Z

	CDF			DØ		
	e	μ	common	1a	1b	common
Statistical	145	205	—	140	70	—
Energy scale	120	50	50	160	80	25
Angle scale	—	—	—	50	40	40
E or p resolution	80	60	—	70	25	10
p_T^W and recoil model	80	75	65	110	95	—
PDF's	50	50	50	65	65	65
QCD/QED corr's	30	30	30	20	20	20
W -width	20	20	20	20	10	10
Backgrounds	10	25	—	35	15	—
Efficiencies	0	25	—	30	25	—
Fitting procedure	10	10	—	5	5	—
Total	230	240	100	270	170	80
Combined	180			150		

Table 3. Errors on M_W in MeV/c^2 .

mass scale. Although only small improvements to the indirect results from LEP/SLC data are expected, the direct measurements of m_W and m_t are expected to improve by factors of 3 – 5 from future measurements [20] at the Tevatron. This would lead to a prediction of the Higgs mass at the level of $\delta m_H/m_H \approx 20\%$.

4.1. Charge Asymmetry in $W \rightarrow \ell\nu$ Events

On average u valence quarks in the proton have higher momentum than d valence quarks. Therefore, W^+ bosons produced via $u\bar{d} \rightarrow W^+$ are boosted predominantly along the proton direction and W^- bosons from $\bar{u}d \rightarrow W^-$ are boosted predominantly along the antiproton direction. This results in an asymmetry in the charged lepton rapidity distribution in $W \rightarrow \ell\nu$ events, defined as

$$A(y_\ell) = \frac{dN^+(y_\ell)/dy_\ell - dN^-(y_\ell)/dy_\ell}{dN^+(y_\ell)/dy_\ell + dN^-(y_\ell)/dy_\ell}$$

where $N^{+(-)}$ is the number of positively (negatively) charged leptons with rapidity y_ℓ . The $(1 \pm \cos\theta)^2$ decay asymmetry from the $V - A$ decay of the W must also be accounted for when studying $A(y_\ell)$. The importance of this measurement is that it is sensitive to the difference in the u and d quark distribution functions at very high Q^2 ($\approx m_W^2$) and low x ($0.007 < x < 0.25$). The measurements therefore constrain the parton distribution functions (PDF's) and are used to reduce the error in m_W due to the uncertainty in the PDF's.

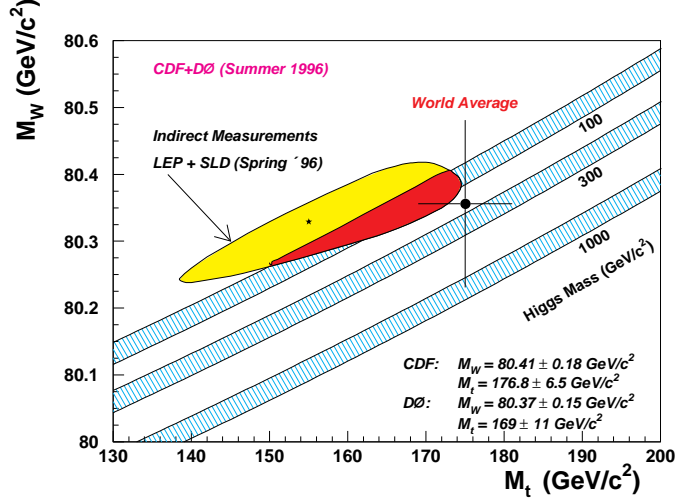


Fig. 9. Direct measurements of m_W and m_t compared with the predictions of the SM for different choices of Higgs boson mass. Also shown is the 1σ allowed region from fits to the LEP and SLC data.

The most recent measurements of this asymmetry from CDF are shown in Figure 10. The data include the run 1a+1b results with a total integrated luminosity of 111 pb^{-1} , utilizing the forward muon toroids and the end plug electromagnetic calorimeter to extend the coverage in rapidity. Also shown are the predictions of the DYRAD NLO Monte Carlo [21] using various parton distribution functions. The uncertainty in the measurement of m_W due to the choice of PDF in the modeling of W events is constrained by selecting only PDF's which show good agreement with the asymmetry data, *i.e.* those for which $|\zeta| < 2$, where

$$\zeta = \frac{\bar{A}_{PDF} - \bar{A}_{data}}{\sigma(\bar{A}_{data})} \quad (1)$$

and \bar{A} is the weighted mean of the asymmetries $A(y_\ell)$. The resulting uncertainty on m_W is $50 \text{ MeV}/c^2$ in the CDF analysis (see Table 3).

5. Conclusions

Recent analyses of data based on the production of W bosons at the Fermilab Tevatron have resulted in precision measurement of the properties of the W . The indirect measurement of the W boson width is $\Gamma(W) =$

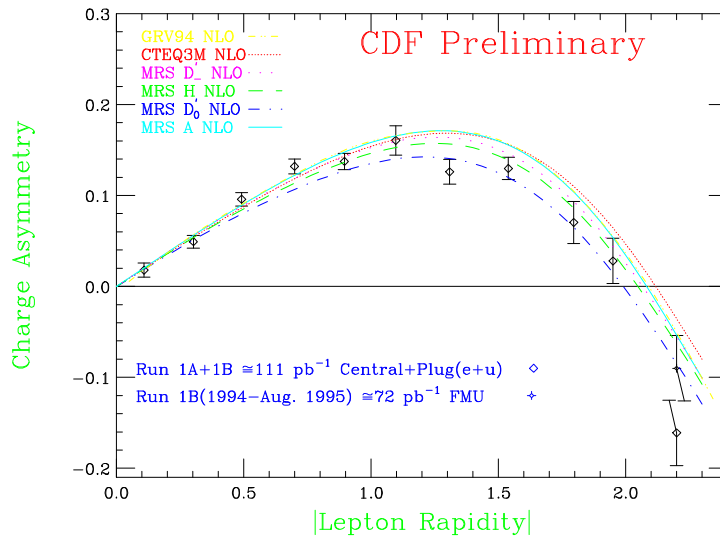


Fig. 10. CDF measurement of the lepton charge asymmetry from $W \rightarrow \ell\nu$ events compared with NLO predictions for different parton distribution functions.

2.062 ± 0.059 GeV (world average, excluding the preliminary run 1b results), corresponding to a precision of 3%. The new world average value of the W mass is $m_W = 80.356 \pm 0.125$ GeV/ c^2 , corresponding to a precision of 0.15%.

New studies of the trilinear gauge boson couplings have also been undertaken. The production of $W\gamma$ and WW events is in agreement with the prediction of the SM, within the experimental sensitivity. The current 95% CL limits on the trilinear coupling parameters are (approximately) $|\Delta\kappa| < 0.9(0.5)$ and $|\lambda| < 0.3(0.3)$ for the $WW\gamma$ coupling assuming $\Lambda = 1.5$ TeV (WWZ coupling assuming $\Lambda = 2.0$ TeV). The measurements provide direct evidence for the existence of the WWZ coupling and show that the photon couples to the SU(2) weak isospin of the W boson as well as to its U(1) electric charge.

The upgraded DØ and CDF detectors will begin running at the Tevatron in 1999. Improvements in the precision in the measurement of the properties of the W boson, coupled with improved measurements of the top quark mass, will yield predictions for the Higgs mass and may provide crucial self consistency tests of the SM.

Acknowledgments

I would like to thank all my colleagues from the DØ and CDF collaborations who helped in preparing my talk and this paper. Particular thanks

to Darien Wood for his useful comments.

REFERENCES

- [1] DØ Collaboration, S. Abachi *et al.* Phys. Rev. Lett. **75**, 1456 (1995).
- [2] CDF Collaboration, F. Abe, *et al.*, Phys. Rev. Lett. **73**, 220 (1994); F. Abe, *et al.*, Phys. Rev. **D52**, 2624 (1995).
- [3] R. Hamberg, W. L. van Neerven and T. Matsuura, Nucl. Phys. **B359**, 343 (1991). W.L. van Neerven and E. B. Zijlstra, Nucl. Phys. **B382**, 11 (1992).
- [4] H. L. Lai *et al.*, Phys. Rev. D **51**, 4763 (1995).
- [5] Particle Data Group, R.M. Barnett *et al.* Phys. Rev. D **54**, 1 (1996).
- [6] J. L. Rosner, M. P. Worah and T. Takeuchi, Phys. Rev. D **49**, 1363 (1994).
- [7] CDF Collaboration, F. Abe *et al.*, Phys. Rev. Lett. **74**, 341 (1995).
- [8] K. Hagiwara, R.D. Peccei and D. Zeppenfeld, Nucl. Phys. **B282**, 253 (1987).
- [9] U. Baur and E.L. Berger, Phys. Rev. D **41**, 1476 (1990).
- [10] DØ Collaboration, S. Abachi *et al.*, Phys. Rev. Lett. **75**, 1034 (1995); S. Abachi *et al.*, FERMILAB-PUB-96/434-E, 1996, Submitted to Phys. Rev. Lett.
- [11] CDF Collaboration, F. Abe *et al.*, Phys. Rev. Lett. **74**, 1936 (1995).
- [12] U. Baur and D. Zeppenfeld, Nucl. Phys. **B308**, 127 (1988).
- [13] CLEO Collaboration, M.S. Alam *et al.*, Phys. Rev. Lett. **74**, 2885 (1995).
- [14] DØ Collaboration, S. Abachi *et al.*, Phys. Rev. Lett. **75**, 1023 (1995).
- [15] CDF Collaboration, F. Abe *et al.*, FERMILAB-PUB-96-311-E, 1996, Submitted to Phys. Rev. Lett.
- [16] J. Ohnemus, Phys. Rev. D **44**, 1403 (1991).
- [17] K. Hagiwara, J. Woodside and D. Zeppenfeld, Phys. Rev. D **41**, 2113 (1990).
- [18] G. Ladinsky and C.-P. Yuan, Phys. Rev. D **50**, 4239 (1994).
- [19] UA2 Collaboration, J. Alitti *et al.*, Phys. Lett. **B276**, 354 (1992); CDF Collaboration, F. Abe *et al.*, Phys. Rev. Lett. **65**, 2243 (1990), Phys. Rev. D **43**, 2070 (1991).
- [20] D. Amidei *et al.*, in “Future Electroweak Physics at the Fermilab Tevatron: Report of the tev_2000 Study Group”, eds. D. Amidei and R. Brock, FERMILAB-PUB-96/082 (1996).
- [21] W. Giele, E. Glover, D.A. Kosower, Nucl. Phys. **B403**, 663 (1993).